



Contents lists available at ScienceDirect

## Computational Materials Science

journal homepage: [www.elsevier.com/locate/commatsci](http://www.elsevier.com/locate/commatsci)

## Material parameters identification: Gradient-based, genetic and hybrid optimization algorithms

B.M. Chaparro<sup>a,\*</sup>, S. Thuillier<sup>b</sup>, L.F. Menezes<sup>c</sup>, P.Y. Manach<sup>b</sup>, J.V. Fernandes<sup>c</sup>

<sup>a</sup>Escola Superior de Tecnologia de Abrantes, Instituto Politécnico de Tomar, Rua de 17 de Agosto de 1808, 2200-370 Abrantes, Portugal

<sup>b</sup>Laboratoire de Génie Mécanique et Matériaux (LG2M), Université de Bretagne-Sud, Rue de Saint Maudé, BP 92116-56321 Lorient cedex, France

<sup>c</sup>CEMUC, Departamento de Engenharia Mecânica, Universidade de Coimbra, Pinhal de Marrocos, 3030-201 Coimbra, Portugal

### ARTICLE INFO

#### Article history:

Received 17 January 2007

Received in revised form 18 March 2008

Accepted 20 March 2008

Available online xxx

#### PACS:

81.40.Lm

62.20.-x

81.70.Bt

81.20.Hy

07.10.-h

62.20.Fe

81.05.-t

#### Keywords:

Plasticity

Anisotropy

Parameter identification

Stamping

Optimization

Yield criteria

Work hardening

### ABSTRACT

This paper presents two procedures for the identification of material parameters, a genetic algorithm and a gradient-based algorithm. These algorithms enable both the yield criterion and the work hardening parameters to be identified. A hybrid algorithm is also used, which is a combination of the former two, in such a way that the result of the genetic algorithm is considered as the initial values for the gradient-based algorithm. The objective of this approach is to improve the performance of the gradient-based algorithm, which is strongly dependent on the initial set of results. The constitutive model used to compare the three different optimization schemes uses the Barlat'91 yield criterion, an isotropic Voce type law and a kinematic Lemaitre and Chaboche law, which is suitable for the case of aluminium alloys. In order to analyse the effectiveness of this optimization procedure, numerical and experimental results for an EN AW-5754 aluminium alloy are compared.

© 2008 Elsevier B.V. All rights reserved.

### 1. Introduction

The numerical simulation of sheet metal forming processes has proven its efficiency and usefulness. In the last twenty years, considerable efforts have been made to improve the numerical methods for solving non-linear problems arising from material behaviour, geometry and friction. Moreover, by means of user-friendly graphical interfaces and due to increasing computer capacity, the use of numerical simulation to analyze the sheet metal forming process has been promoted at an industrial scale. Despite the advances in this domain, the final result of the simulation of metal forming processes depends greatly on the limitations of the constitutive material behaviour model, used in the simulations [1,2]. In fact, various types of models can be used, according

to their ability to explain and/or predict the details of the plastic behaviour during a given deformation process. Simple models of isotropic hardening can give an acceptable estimate of the drawing forces occurring during the process and are widely used in industry [3]. However, more sophisticated models, involving for instance non-linear kinematic hardening and more refined yield criteria models, give improved evaluation of the evolution of every deformation process [4–7]. Generally, these models have a large number of parameters, which increases the amount and type of experimental tests necessary for their evaluation. Moreover, the results of the parameter evaluation are often inconsistent [8–10].

The identification of the material parameters, for a given constitutive model, can be seen as an inverse formulation. In this context, the key idea is to simulate the performed experiment, trying to adapt material parameters in order to numerically obtain the same results as the experimental ones [11,12]. This approach consists of an optimization problem where the objective function is to mini-

\* Corresponding author. Tel.: +351 241 379 500; fax: +351 241 361 175.

E-mail address: [bruno.chaparro@dem.uc.pt](mailto:bruno.chaparro@dem.uc.pt) (B.M. Chaparro).

mize the gap between the experimental and the numerical results. The optimization variables are the material parameters that appear in the constitutive model. To solve this problem one can use different methods that can be divided mainly into three groups:

1. Derivative-free search algorithms.
2. Gradient-based algorithms.
3. Evolutionary algorithms.

The derivative-free algorithms, also called direct search algorithms, are generally based on simple strategies and do not require the calculation of derivatives. Their simplicity is their main attribute. However, direct search algorithms undergo the problem of converging to local minimums, and are also somehow user-dependent. The convergence of these algorithms is very time-consuming and involves the comparison of each trial solution with the best previous solution. One can refer to several methods based on direct search strategies namely: pattern search [13], Rosenbrock [14], simplex [15] and Powell [16]. These methods remain popular because of their simplicity, flexibility and reliability.

The gradient-based algorithms usually converge quickly in the vicinity of the solution, and are therefore very interesting in terms of rapidity. However, they have some limitations, being strongly dependent on user skills, due to the need to choose the initial trial solutions. Also, they can easily fall to local minimums, mainly when the procedure is applied to multi-objective functions, as is the case with material parameter identification. The requirement of derivative calculation makes these methods non-trivial to implement. One can mention a large number of optimization gradient-based methods such as the Steepest Descent Method, the Newton method or several Quasi-Newton Methods [17–20].

An *evolutionary algorithm* is a generic definition used to indicate any population-based optimization algorithm that makes use of some mechanism to improve the initial solutions. The trial solutions to the optimization problem are individuals in a population. Evolution of the population takes place after the repeated application of the genetic operators (reproduction, mutation, recombination, etc.). These algorithms have become very popular in recent years, mainly because of the increase in computer calculation speed that leads to optimized results in an acceptable time. Moreover, it is generally believed that evolutionary algorithms perform consistently well across all types of problems, which is evidenced by their success in fields such as engineering, art, biology, economics, genetics, robotics, social sciences and others. Although they are robust methods, their convergence is very time-consuming, and they must be considered as sub-optimal algorithms, as for continuous variable optimization the global minimum of the objective function is not guaranteed. Anyway, local minima are generally avoided and the final solution is in the vicinity of the global minimum. Genetic algorithms are the most popular type of evolutionary algorithms that make use of biological evolutionary analogies to improve the initial set of solutions.

In conclusion, these three types of approaches to variable optimization can be used to solve the problem of determining the material parameters of a given constitutive model. All the algorithms have advantages and drawbacks. However, one can produce hybrid algorithms combining the advantages of each approach, e.g. robustness of the genetic algorithm and performance of the gradient-based algorithm. Generally speaking, if the constitutive model is relatively simple e.g. isotropic hardening described by a power law and an isotropic Hill'48 [21] yield criterion, the identification is relatively easy to perform, whenever the available experimental data is sufficient. As the complexity of constitutive models increases, identification be-

comes non-trivial, and generally demands user skills. To explore and identify the problems and difficulties that can arise during the parameter identification procedure, this paper makes use of two different algorithms, a gradient-based and an evolutive algorithm, to identify the material parameters of the constitutive equations model in the case of a 1 mm thick sheet of EN AW-5754-O aluminium alloy, used in the automotive industry. A set of experimental results was obtained from tension and both monotonic and Bauschinger shear tests. The Barlat'91 [22] yield criterion is considered. A Voce type equation [23] with kinematic hardening component described by the Lemaitre and Chaboche law [24] is used.

The paper is structured as follows. In Section 2, the constitutive equations are briefly illustrated. In Section 3 the parameter identification problem and the two algorithms used are presented. In Section 4 the experimental tests are described. In Section 5 the results of the parameters identified are discussed. And Section 6 sums up the main conclusions of this work.

## 2. Constitutive equations

The YLD91 yield criterion was proposed by Barlat et al. [22,25] and was written from previous isotropic criterion defined by Hershey and Hosford [26,27]. It can be written as follows:

$$\phi = |S_1 - S_2|^m + |S_2 - S_3|^m + |S_3 - S_1|^m = 2\bar{\sigma}^m \quad (1)$$

where  $S_1$ ,  $S_2$  and  $S_3$  are the principal values of the isotropic plastic equivalent deviatoric stress tensor  $\mathbf{S}$ , which is obtained from the Cauchy stress tensor  $\boldsymbol{\sigma}$  by a linear transformation;  $m$  is an exponent which can be considered equal to, respectively, 6 for BCC and 8 for FCC materials [28] and  $\bar{\sigma}$  is the equivalent stress. The linear transformation used to calculate the isotropic plastic equivalent (IPE) stress tensor  $\mathbf{S}$  is

$$\mathbf{S} = \mathbf{L} : \boldsymbol{\sigma} \quad (2)$$

where  $\mathbf{L}$  is the linear transformation tensor, defined for orthotropy [29] by

$$\mathbf{L} = \begin{bmatrix} (c_2 + c_3)/3 & -c_3/3 & -c_2/3 & 0 & 0 & 0 \\ -c_3/3 & (c_3 + c_1)/3 & -c_1/3 & 0 & 0 & 0 \\ -c_2/3 & -c_1/3 & (c_1 + c_2)/3 & 0 & 0 & 0 \\ 0 & 0 & 0 & c_4 & 0 & 0 \\ 0 & 0 & 0 & 0 & c_5 & 0 \\ 0 & 0 & 0 & 0 & 0 & c_6 \end{bmatrix} \quad (3)$$

where  $c_1$ ,  $c_2$ ,  $c_3$ ,  $c_4$ ,  $c_5$  and  $c_6$  are the parameters that describe the anisotropy. When all parameters  $c_i$  ( $i = 1$  to 6) are equal to one and  $m = 2$ , the YLD91 criterion reduces to the von Mises yield criterion. The parameters to be identified in this model are  $c_1$ ,  $c_2$ ,  $c_3$  and  $c_6$ . The parameters  $c_4$  and  $c_5$ , the identification of which requires shear tests to be performed in the sheet thickness, are kept constant and equal to isotropic values ( $c_4 = c_5 = 1$ ); this is because the experimental database does not involve such strain paths. As above mentioned, an exponent value of  $m = 8$  is used [28], which is coherent with the behaviour of FCC materials such as aluminium alloys.

The yield surface is described by the equation:

$$\phi = \bar{\sigma} - Y = 0 \quad (4)$$

where  $Y$  is the yield stress that takes as initial value  $Y_0$ . The yield stress evolution is given by the Voce law [23], defined as:

$$\dot{Y} = C_Y (Y_{\text{sat}} - Y) \dot{\epsilon}^p \quad (5)$$

where  $\dot{\epsilon}^p$  is the equivalent plastic strain rate and  $C_Y$  and  $Y_{\text{sat}}$  are material parameters to be identified. This model is used in the simulation of materials whose behaviour presents saturated hardening.

In order to take into account kinematic hardening, the tensor  $\mathbf{S}$  becomes:

$$\mathbf{S} = \mathbf{L} : (\boldsymbol{\sigma} - \mathbf{X}) \quad (6)$$

where the backstress tensor ( $\mathbf{X}$ ) can be described by the non-linear with saturation law proposed by Lemaître and Chaboche [24]:

$$\dot{\mathbf{X}} = C_x \left[ X_{\text{sat}} \left( \frac{\boldsymbol{\sigma}' - \mathbf{X}}{\bar{\sigma}} \right) - \mathbf{X} \right] \dot{\bar{\epsilon}}^p \quad (7)$$

where  $C_x$  and  $X_{\text{sat}}$  are material parameters to be identified.  $\boldsymbol{\sigma}'$  is the deviatoric part of the stress tensor.

The above described anisotropic yield criterion and hardening laws were chosen because they correspond to the most suitable set of phenomenological constitutive laws to describe the aluminium alloy behaviour.

### 3. Parameter identification

It is not possible to experimentally determine the behaviour of the material for all possible strain paths and therefore a limited number of tests are usually considered, representative of the strain paths encountered during the deep drawing process. To characterize the behaviour of deep drawing quality metals, the most widely experimental tests used are tensile, shear and equibiaxial tensile tests. In case of constitutive laws involving kinematic hardening, reverse strain paths have to be taken into account, such as tension-compression tests [30], bending-unbending tests [31,32] or planar Bauschinger shear tests [33,34]. The mechanical behaviour of a material is then modelled, for use in numerical simulations of the forming process, by means of the parameters identified from the available experimental data.

The experimental database provides information for specific strain paths, which allows parameter identification by minimizing the difference between the numerical parameter optimization approach (for the constitutive model used) and the experimental results. The material parameter identification is then a minimum error problem, where the error can be defined as the difference between the results of the optimization approach and the experimental data. The error (or cost) function can be expressed as:

$$F(\mathbf{A}) = \frac{1}{N} \sum_{i=1}^N [P_i^{\text{num}}(\mathbf{A}) - P_i^{\text{exp}}]^2 \quad (8)$$

where  $F(\mathbf{A})$  is the error function,  $\mathbf{A}$  the set of the parameters for the constitutive model,  $N$  the number of experimental points;  $P_i^{\text{num}}(\mathbf{A})$  and  $P_i^{\text{exp}}$  are the numerical and experimental values at a given instant.

#### 3.1. Gradient-based optimization method

The derivative or gradient-based algorithm used in this study was developed by Pilvin and has already been largely discussed [8]. It is briefly reviewed here. The algorithm thus obtained was introduced into SiDoLo software. A fundamental issue regarding the optimization using second order gradient-based optimization methods, such as this one, is the initial guess for the set of parameters; if it is not carefully chosen, the iterative method can lead to convergence difficulties. In order to accelerate the convergence, two gradient-based methods were combined [35,36]. A steepest descent method is used for determination at the beginning of the optimization procedure and the Levenberg–Marquardt method [37,38] is used to accelerate the convergence after the initial stages of the optimization process [39]. This second order gradient-based optimization method guarantees the convergence, at least to a local minimum and is, in general, the most widely used optimization algorithm [8] for identification tasks. In order to integrate the

**Table 1**

Diagram of the genetic algorithm used

- |   |
|---|
| 1 Generate the initial population.  |
| 2 Start GA iterations $n = 1$ to $n_{\text{max}}$ :                         |
| 2.1. Evaluate the fitness function for all solutions                        |
| 2.2. Select the solutions to the mating pool                                |
| 2.3. Combine solutions by a crossover technique                             |
| 2.4. Apply the mutation operator  |
| 2.5. Apply elitism strategy   |
| 3 Stop iteration process if $n_{\text{max}}$ is reached or return to step 2 |

internal variable equations, the gradient-based method implemented in the program SiDoLo uses Runge–Kutta explicit numerical integration.

#### 3.2. Evolutive optimization algorithm

In order to perform the material parameter identification an algorithm based on the genetic evolutive scheme was also implemented. The genetic algorithm (GA) is a selective random search algorithm designed to achieve a global optimum within a large space of solutions, as proposed by Holland [40]. The initial solutions (population) of the GA algorithm are usually randomly generated. If some adequate quality solutions are known then it is possible to include them in the initial population, which is known as a seeding procedure. For instance, in this study it was possible to insert the solutions obtained with the isotropic von Mises yield criterion in the initial population. Then, for all the individuals the fitness function is calculated. This fitness function measures the robustness of each solution. Therefore a fitness-dependent technique is used to select the parents for the next population from the current one, setting them in the mating pool. This acts as a natural selection process where the strongest individuals have more probability of leaving their genetic information to the next generation. The next generation of solutions is obtained by a crossover technique from the individuals in the mating pool. In this study a single point crossover is used to perform this task. In order to ensure genetic diversity, a mutation operator is used. This is related to the exploration and exploitation balance that should be present in the convergence of the GA algorithm [41]. A way to increase this “converging pressure” is to maintain part of the population; this procedure is referred to as an elitism strategy. This algorithm is repeated until the end condition is reached. The diagram of the optimization problem, using the genetic algorithm is shown in Table 1.

### 4. Experimental data

The material used was an EN AW-5754-O aluminium alloy. The samples for mechanical tests were cut from a 1 mm thick sheet. Uniaxial tensile tests and simple shear tests were performed at 0°, 45° and 90° to the rolling direction (RD). Both types of tests were carried out at an equivalent strain rate of  $8 \times 10^{-4} \text{ s}^{-1}$ . Tensile samples have a gauged area of  $150 \times 20 \text{ mm}^2$ . A local strain gauge, at the centre region of the sample, coupled with a CCD camera, allows the calculation of longitudinal and transverse logarithmic strains. The true stress is calculated from the load by assuming an isochoric plastic transformation. Simple shear samples have a gauged area of  $4.5 \times 50 \text{ mm}^2$  and the local shear strain  $\gamma$ , at the centre region of the sample, is also recorded by a CCD camera. To identify the kinematic hardening, Baushinger-type shear tests were carried out in the RD direction. They consist of a loading of the sample up to a maximum shear value ( $\gamma = 0.1, 0.2$  and  $0.3$  in this study) followed by unloading and reversal of the loading direction. The experimental data obtained for the 1 mm thick sheets of

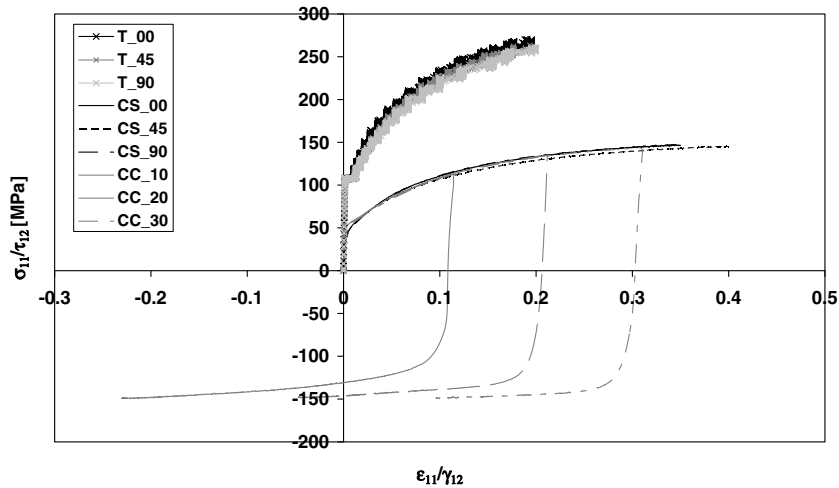


Fig. 1. Experimental results obtained for the EN AW-5754-O aluminium alloy: tensile and shear tests at 0°, 45° and 90° to the rolling direction (T 00, T 45 and T 90 for the tensile tests and CS 00, CS 45 and CS 90 for the shear tests) and Baushinger (shear) tests obtained at 0° to the rolling direction after 10, 20 and 30% of pre-deformation in shear (CC 00 10, CC 00 20 CC 00 30).

Table 2

Experimental data obtained for the EN AW-5754-O aluminium alloy

Angle with RD (°)	r-value	Initial yield stress ( $\sigma_z$ ) (MPa)
0	0.707	107.6
45	0.611	105.5
90	0.536	107.0

the EN AW-5754-O aluminium alloy is shown in Fig. 1. This material exhibits a Portevin–Le Châtelier (PLC) effect, which is responsible for the serrations observed on the stress–strain curves in tension.

Table 2 presents the experimental plastic anisotropy coefficients,  $r$ , and the yield stresses,  $\sigma_z$ , obtained in tension in the sheet plane for 0°, 45° and 90° to RD. The plastic anisotropy coefficients are determined by fitting the results of the plastic strain in width versus the plastic strain in thickness up to 0.20 of longitudinal strain. It can be seen that this material exhibits weak planar anisotropy, particularly in the stress–strain curve.

### 5. Identification results

The identification procedure is a minimization of the cost function over all the tests in the database (Eq. (8)). For the gradient-based algorithm, an initial set of parameters was chosen and the calculation was stopped after 200 iterations or after a stagnation of the cost function. For the evolutive algorithm, all identifications were performed considering a crossover probability of 75% and a mutation probability of 5%. The population was 70 individuals and 120 iterations were performed. The elitism strategy keeps the 6 best elements in each population.

The yield stress parameters for the YLD91 criterion obtained with the two different approaches are shown in Table 3. In this table the label SiDoLo refers to the results obtained with the gradi-

Table 3

Identified parameters obtained for the YLD91 model with SiDoLo and with DD3MAT

	$c_1$	$c_2$	$c_3$	$c_6$	$m$
SIDOLO (Set 1)	1.275 (1.0)	1.096 (1.0)	0.896 (1.0)	0.998 (1.0)	8
DD3MAT	1.121	1.029	0.933	0.981	8

The initial values are given in brackets.

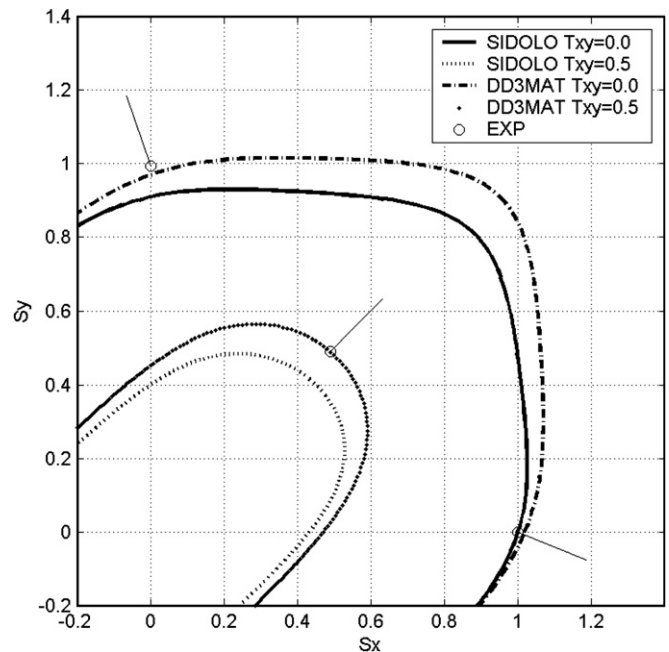


Fig. 2. Numerical results for the yield stress surface of the EN AW-5754-O aluminium alloy. Experimental results obtained in tension at 0, 45 and 90° with RD direction. The numerical results presented were obtained with SiDoLo (Set 1) and with DD3MAT.

ent-based program. For this case, the initial set of parameters is indicated in brackets. The parameters obtained with the evolutive program are referred to as DD3MAT results. Fig. 2 presents the yield surface obtained with the two different approaches. Projections of the yield surface are performed in the normal stress plane  $\sigma_{xx} - \sigma_{yy}$  for  $\tau_{xy} = 0$  and  $\tau_{xy} = 0.5$ , all values being normalized by the yield stress obtained in tension in the rolling direction, where  $ox$  is the rolling direction and  $oy$  is the transverse direction. The normalized experimental results are also plotted, i.e. the yield stress values, obtained at 0°, 45° and 90° with respect to RD. These points are represented by small circles and the respective normal directions to the yield surface in each experimental point are drawn, as calculated from the experimental  $r$  values (Table 2). It is possible to observe slight differences in the shape of the yield surfaces for both

**Table 4**  
Identified parameters for the mixed hardening model with SiDoLo

		$Y_0$ (MPa)	$Y_{sat}$ (MPa)	$C_Y$
Voce	Set 1	51.2 (107.6)	153.9 (200.0)	11.91 (50.0)
	Set 2	128.7 (107.6)	193.4 (200.0)	6.9 (5.0)
	Set 3	85.8 (107.6)	182.7 (200.0)	16.2 (50.0)
		$C_X$	$X_{sat}$ (MPa)	
NLSL	Set 1	111.6 (10.0)	73.0 (10.0)	
	Set 2	1.24 (1.0)	1.02 (1.0)	
	Set 3	671.8 (1000.0)	2.24 (1.0)	

The initial values are given in brackets.

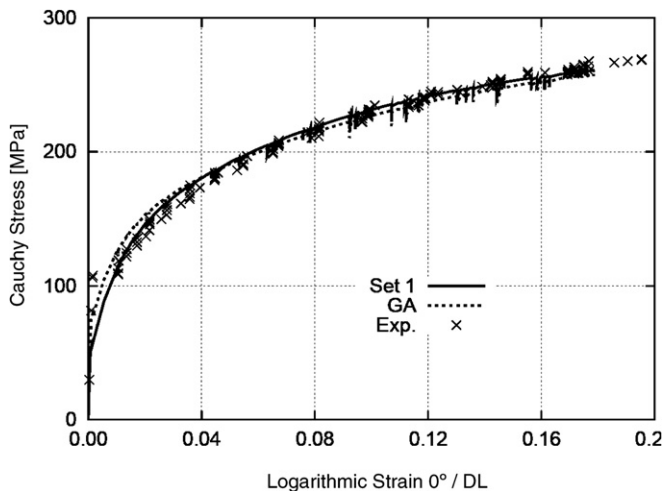
identifications. The main differences are observed for the equibiaxial stretching strain path. When comparing the directions of the normal to the yield surface with the experimental results, some small differences are observed, particularly for the case of the gradient-based program. The parameter identification results could be improved by means of experimental data concerning the equibiaxial stretching strain path, i.e. using bulge or an approximation to allow the biaxial data to be accessed through tensile results in the thickness direction as proposed, for example, by Green [42] and Tong [43].

Table 4 presents the identified mixed hardening coefficients, for Voce law and the non-linear with saturation law proposed by Lemaitre and Chaboche (NLSL), obtained with SiDoLo. In order to test the influence of the initial set of parameters within the derivative-based algorithm, three cases (number 1, 2 and 3) were tested. For all identifications, the initial value of  $Y_0$  was kept equal to experimental yield stress in the rolling direction, and the value of  $Y_{sat}$  was 200 MPa (see Table 4); the other initial values are also shown in Table 4. The initial YLD91 parameters were set equal to

**Table 5**  
Identified parameters for the mixed hardening model with DD3MAT

Voce	$Y_0$ (MPa) (10,150)	$Y_{sat}$ (MPa) (100,250)	$C_Y$ (1,15)
	73.2	146.8	9.6
NLSL	$C_X$ (1,150)		$X_{sat}$ (MPa) (10,120)
	117.5		60.5

The limit values are given in straight brackets.



**Fig. 3.** Experimental and numerical results obtained for the tensile test performed at 0° to RD. The numerical results presented were obtained with SiDoLo (Set 1) and with DD3MAT.

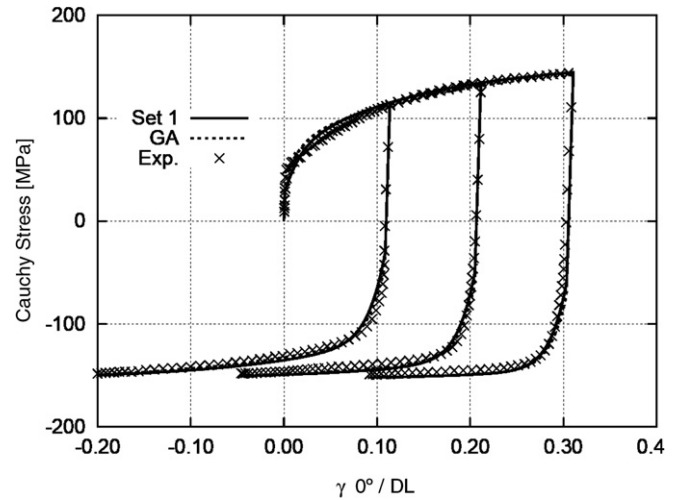


**Fig. 4.** Experimental and numerical results obtained for the cyclic tests (10, 20 and 30% of prestrain) performed at 0° to RD. The numerical results presented were obtained with SiDoLo (Set 1) and with DD3MAT.

1.0 (see also Table 3). Table 4 shows large differences between the final results obtained with the different sets. The results obtained with sets 2 and 3 were not kept as valid once the cost function remained in the vicinity of 300, whereas with the set 1 the cost function reduces to near 150.

Table 5 shows the parameters obtained with the evolutive algorithm, which are almost identical for several runs. The limit values imposed for each parameter in the identification are also shown in this table (values in square brackets).

The mechanical behaviour of the material is well described using the set 1 of parameters in Table 4, (obtained with the derivative-based method) and the results presented in Table 5 (obtained with the genetic algorithm). This is shown in Figs. 3 and 4, which show the results obtained for tensile tests in the RD as well as monotonic and Bauschinger shear tests for both identification methods. Both numerical results exhibit close agreement with experimental ones even in the reverse paths.

### 5.1. Improvement of the identification strategy

In order to improve the overall optimization procedure, a hybrid scheme was developed. The hybrid algorithm was obtained using first the genetic algorithm to obtain a point near the minimum,

**Table 6**  
Identified parameters for the yield surface with the hybrid scheme (DD3MAT + SiDoLo)

	$c_1$	$c_2$	$c_3$	$c_6$	$m$
SiDoLo (Set 4)	1.303	1.128	0.938	1.031	8

Values given in Table 3 (DD3MAT) and Table 5 were used as initial parameters.

**Table 7**  
Identified parameters for the mixed hardening model with the hybrid scheme (DD3MAT + SiDoLo)

Voce	$Y_0$ (MPa)	$Y_{sat}$ (MPa)	$C_Y$
	61.4	156.1	11.8
NLSL	$C_X$		$X_{sat}$ (MPa)
	87.3		68.3

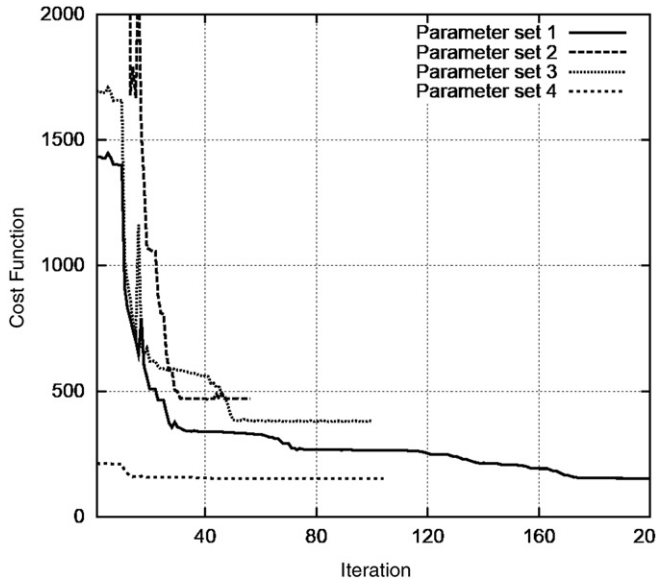


Fig. 5. Evolution of the cost function with iterations for the identifications performed with the derivative-based method (Sets 1, 2 and 3) and the identification performed with the hybrid identification scheme (DD3MAT + SiDoLo).

and then use the derivative-based, as a local search algorithm, to achieve the minimum. With this strategy it is possible to combine the advantages of the derivative and the evolutive algorithms. Tables 6 and 7 present the results obtained with this scheme for the parameters of the yield surface criterion and for the mixed hardening model, respectively. This new set of numerical results is referred to below as set 4. Fig. 5 presents the evolution of the identification error with the iteration (cost function), for all optimizations performed with the derivative based program (sets 1, 2 and 3) as well as for the optimization performed using as an initial set the results obtained with the hybrid algorithm (set 4). From this figure it can be observed that the derivative-based algorithm sometimes converges to a local minimum, as has been previously mentioned. The decrease in the cost function at the beginning of the identification for set 4 is due to the sub-optimal nature of the GA algorithm [40]. However, when using the result of the genetic algorithm as initial set for the gradient-based algorithm, convergence is rapidly reached around a high-quality set of parameters. The cost function values obtained for sets 1 and 4 are 151.94 and 150.33, respectively. The hybrid algorithm gives a better solution than those obtained with the derivative-based algorithms.

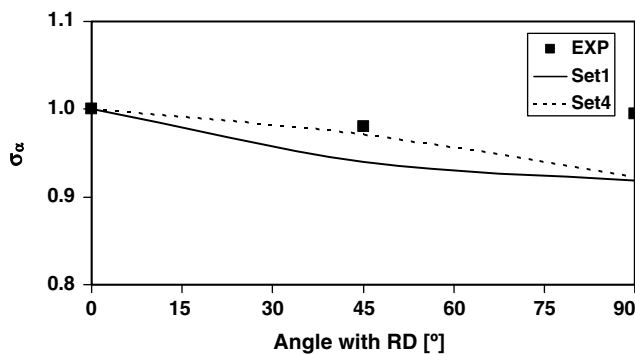


Fig. 6. Experimental and numerical results of the variation in plane of the initial values of the uniaxial yield stress obtained with the derivative-based and the hybrid algorithm.

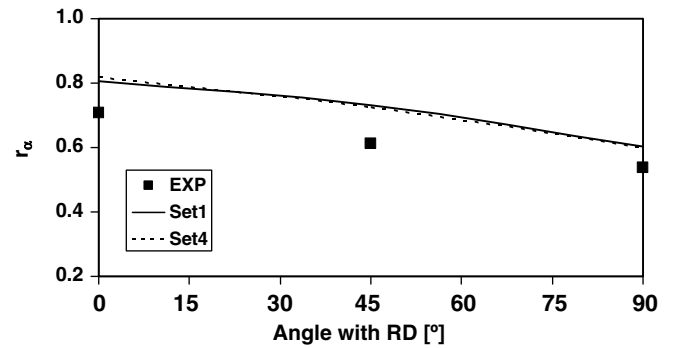


Fig. 7. Experimental and numerical results of the variation in plane of the initial values of the Lanckford coefficients obtained with the derivative-based and the hybrid algorithm.

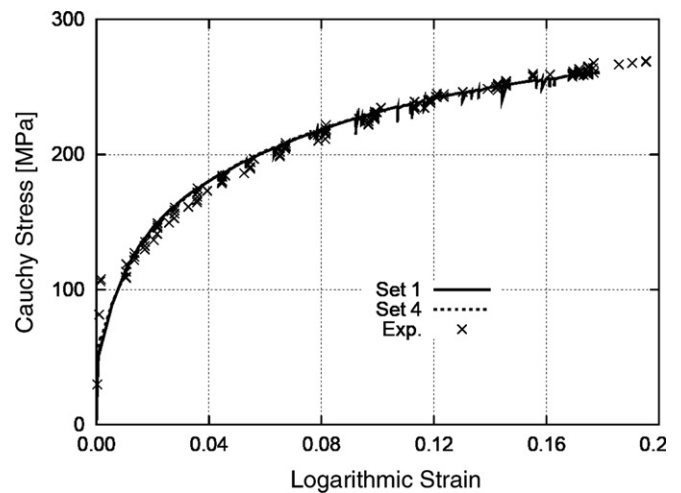


Fig. 8. Experimental and numerical results for the tensile test obtained with the derivative-based and the hybrid algorithm in the rolling direction.

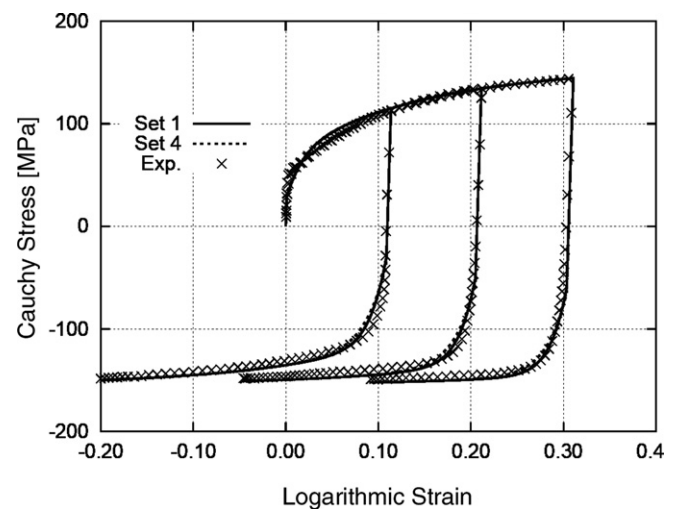
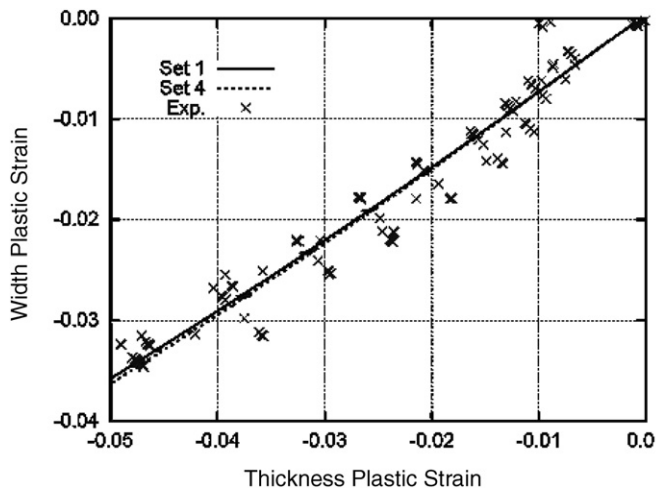


Fig. 9. Experimental and numerical results for the cyclic test obtained with the derivative-based and the hybrid algorithm in the rolling direction.

Figs. 6 and 7 show the experimental and numerical results obtained with set 1 and 4 for the variation in plane of the initial values of the uniaxial yield stress and Lanckford coefficients. Figs.



**Fig. 10.** Experimental and numerical results obtain for width plastic strain versus thickness plastic strain in tension, in the rolling direction. The numerical results presented were obtained for sets 1 and 4.

8–10 show the experimental and numerical results obtained with set 1 and 4 for tensile tests, cyclic tests and width versus thickness plastic strains, respectively. It is possible to conclude from these figures that both sets are representative of the experimental behaviour, although the constitutive parameters for these two sets are slightly different (cf. Tables 3, 4, 6 and 7). This is due to the fact that the mechanical description, particularly the isotropic–kinematic hardening components, depends on the connection between the different laws. This implies a difficult optimization task, revealed by the different sets obtained for the derivative-based method presented in Table 4. The hybrid scheme is clearly more robust.

The CPU time spent for identification of all parameters was 60 and 30 min using the genetic algorithm and the derivative-based algorithm, respectively (the computer used was a Pentium IV 3.0 GHz). The use of the hybrid algorithm leads to a lower calculation time, taking 25 min for the entire identification procedure. Indeed, the number of generations of the genetic algorithm can be greatly reduced and, as the solution is near the optimal solution, the derivative-based methods converge in few steps.

## 6. Conclusions

This paper presents a comparison of optimization strategies for performing material parameter identification of an EN AW-5754-O sheet aluminium alloy. Tensile and shear tests were performed in order to obtain an experimental database on this material. The constitutive model used to describe the material behaviour is a phenomenological model composed of the YLD91 orthotropic plasticity criterion, the isotropic hardening law of Voce type and the non-linear kinematic hardening of Lemaitre and Chaboche. Two optimization algorithms are used: a genetic algorithm and a derivative-based algorithm. It is shown that both algorithms are able to fit the experimental behaviour even though the traditional problems of each algorithm have been encountered: large calculation times and sub-optimal problems for the GA and the inability of the derivative-based algorithm to avoid local minima. To improve the optimization procedure, a hybrid strategy is proposed which combines the advantages of both methods, i.e. firstly, the robustness of the genetic algorithm is used to reach the vicinity of the global minimum and then the precision of the derivative-based algorithm is used to reach the optimal set of parameters. With this method, it is shown that by performing a fine parameter optimization, it has been possible to fit most of the macroscopic effects

observed in this material, using the constitutive models mentioned above.

## Acknowledgement

The authors are grateful to the Portuguese Foundation for Science and Technology (FCT) who financially supported this work, through the Program POCI 2010 (Portuguese Government and FED-ER). One of the authors, B.M. Chaparro, was supported by a grant for scientific research from Portuguese Government, through the Program PRODEP. This support is gratefully acknowledged.

## References

- [1] S. Bouvier, J.L. Alves, M.C. Oliveira, L.F. Menezes, *Computational Materials Science* 32 (2005) 301–315.
- [2] Z. Dongjuan, C. Zhenshan, R. Xueyu, L. Yuqiang, *Computational Materials Science* 38 (2006) 256–262.
- [3] J. Cao, M.F. Shi, T.B. Stoughton, C.-T. Wang, L. Zhang, *The Numisheet 2005 Benchmark Study*, in: *Proceedings of NUMISHEET 2005*, Detroit, MI, USA, 2005.
- [4] A. Makinouchi, Recent developments in sheet metal forming simulation, simulation of materials processing – theory, methods and applications, in: K. Mori (Ed.), *Proceedings of NUMIFORM 2001*, Toyohashi, Japan, 3–10, 2001.
- [5] B.M. Chaparro, M.C. Oliveira, J.L. Alves, L.F. Menezes, *Materials Science Forum* 455–456 (2004) 717–722.
- [6] F. Roters, *Computational Materials Science* 32 (2005) 509–517.
- [7] A. Bahrami, S.H.M. Anijdan, H.R.M. Hosseini, A. Shafyei, R. Narimani, *Computational Materials Science* 34 (2005) 335–341.
- [8] G. Cailletaud, P. Pilvin, *Inverse Problems in Engineering* 79–86 (1994) 1994.
- [9] T. Furukawa, G. Yagawa, *International Journal of Numerical Methods in Engineering* 40 (1997) 1071–1090.
- [10] T. Furukawa, T. Sugata, S. Yoshimura, M. Hoffman, *Computer Methods in Applied Mechanics and Engineering* 191 (2002) 2235–2260.
- [11] M. Springmann, M. Kuna, *Computational Materials Science* 32 (2005) 544–552.
- [12] B. Kowalski, C.M. Sillars, M. Pietrzyk, *Computational Materials Science* 35 (2006) 92–97.
- [13] W.C. Davidon, Variable metric method for minimization, Argonne National Laboratory Research and Development, Report 5990, 1959.
- [14] H.H. Rosenbrock, *Computational Journal* 3 (1960) 175–184.
- [15] W. Spendley, G.R. Hext, F.R. Himsworth, *Technometrics* 4 (1962) 441–461.
- [16] M.J.D. Powell, *Computational Journal* 7 (1964) 155–162.
- [17] M.S. Bazaraa, H.D. Sherali, C.M. Shetty, *Nonlinear Programming: Theory and Algorithms*, Wiley, New York, 1973.
- [18] R. Fletcher, *Practical Methods of Optimization*, Wiley, New York, 1987.
- [19] M.T. Heath, *Scientific Computing: An Introduction Survey*, McGrawHill, New York, 1997.
- [20] J. Nocedal, S. Wright, *Numerical Optimization*, Springer, New York, 1999.
- [21] R. Hill, *The Mathematical Theory of Plasticity*, Clarendon Press, Oxford, 1950.
- [22] F. Barlat, D.J. Lege, J.C. Brem, *International Journal of Plasticity* 7 (1991) 693–712.
- [23] E. Voce, *Journal of the Institute of Metals* 74 (1948) 537–562.
- [24] J. Lemaitre, J.L. Chaboche, *Mechanics of Solids Materials*, Cambridge University Press, Cambridge, 1985.
- [25] F. Barlat, Y. Maeda, K. Chung, M. Yanagawa, J.C. Brem, Y. Hayashida, D.J. Lege, K. Matsui, S.J. Murtha, S. Hattori, R.C. Becker, S. Makosey, *Journal of Mechanics and Physics of Solids* 45 (1997) 1727–1763.
- [26] A.V. Hershey, *Journal of Applied Mechanical Transactions (ASME)* 21 (1954) 241–249.
- [27] W.F. Hosford, *Journal of Applied Mechanics* 39 (1972) 607–609.
- [28] R.W. Logan, W.F. Hosford, *International Journal of Mechanical Sciences* 22 (1980) 419–430.
- [29] A.P. Karafillis, M.C. Boyce, *Journal of the Mechanics of Physics of Solids* 41 (1993) 1859–1886.
- [30] F. Yoshida, T. Uemori, K. Fujiwara, *International Journal of Plasticity* 18 (2002) 633–659.
- [31] F. Yoshida, M. Urabe, V.V. Toropov, *International Journal of Mechanical Sciences* 40 (1998) 237–249.
- [32] M. Brunet, F. Morestin, S. Goderaux, *Journal of Engineering Materials and Technology* 123 (2001) 378–383.
- [33] P.Y. Manach, D. Favier, *Materials Science and Engineering A222* (1997) 45–57.
- [34] S. Bouvier, H. Haddadi, P. Levée, C. Teodosiu, *Journal of Materials Processing Technology* 172 (2006) 96–103.
- [35] A. Andrade-Campos, S. Thuillier, P. Pilvin, F. Teixeira-Dias, On the estimation of material parameters for internal variable thermoelastic–viscoplastic constitutive models: gradient-based and GA optimization algorithms, in: *Proceedings of Computational Mechanics WCCM VI in conjunction with APCOM'04*, Beijing, China, Tsinghua University Press and Springer-Verlag, 2004.

- [36] K.M. Zhao, J.K. Lee, *Communications in Numerical Methods in Engineering* 20 (2004) 105–108.
- [37] K. Levenberg, *Quarterly of Applied Mathematics* 2 (1944) 164–168.
- [38] D. Marquardt, *SIAM Journal of Applied Mathematics* 11 (1963) 431–441.
- [39] J.W. Ju, J.C. Simo, K.S. Pister, R.L. Taylor, A parameter estimation algorithm for inelastic material models, in: *International Conference on Constitutive Laws for Engineering Materials*, Tucson, Arizona, 1987, pp. 1233–1239.
- [40] J.H. Holland, *Adaptation in Neural and Artificial Systems*, University of Michigan Press, Ann Arbor, 1975.
- [41] T. Back, U. Hammel, H.P. Schwefel, *IEEE Transactions on Evolutionary Computation* 1 (1997) 3–17.
- [42] D.E. Green, K.W. Neale, S.R. MacEwen, A. Makinde, R. Perrin, *International Journal of Plasticity* 20 (2004) 1677–1706.
- [43] W. Tong, *International Journal of Plasticity* 22 (2006) 497–535.